
Multimedia Tools and Applications, 13, 307–332, 2001

Feedback Flow Control with Hysteresial Techniques for Multimedia Retrievals

JUAN C. GUERRI jcguerri@dcom.upv.es
MANUEL ESTEVE mesteve@dcom.upv.es
CARLOS PALAU cpalau@dcom.upv.es
VICENTE CASARES vcasares@dcom.upv.es
Department of Communications, Polytechnic University of Valencia, Valencia, Spain

Abstract. The objective of this paper is to demonstrate the advantages of using hysteresial techniques in flow control mechanisms. The work scenario consists of a server transmitting video information to a group of clients. Each client stores the information in a buffer and then plays it back at a set consumption rate. To avoid "overflow" or "underflow" in the buffer, the client sends control messages (feedbacks) to the server which order adjustments in the transmission rate. Hysteresial techniques allow the minimization of this signaling traffic, even when there are rapid fluctuations in the buffer occupation. As a first step, an analytical model is developed using Markovian processes. This produces expressions of the most relevant parameters and allows the evaluation of the proposed flow control mechanism. The Markovian model has been compared with the performance of a multimedia application for video distribution, running in a real scenario. The results show that the model represents qualitatively the real scenario and consequently validates the model usefulness.

Keywords: feedback flow control, hysteresial, synchronization, Markov models

1. Introduction

Temporal synchronization and flow control are basic features for providing and guaranteeing a satisfactory quality of service in multimedia communication systems [18]. The former refers to temporal relationships between different media objects (video, audio, text, etc.). Flow control allows a continuous playback, avoiding "underflows" and "overflows" in the reception buffer of the client.

Temporal synchronization can be separated into *intra-object synchronization* and *inter-object synchronization*. The former refers to the temporal relationships between several LDU's (Logical Data Unit) [16] of the same information object. An example is the temporal relationship between several frames of the same video sequence. For video, with a rate of 25 frames per second, one frame should be represented every 40 ms in the video visualization display. Figure 1 shows this synchronization requirement. Inter-object synchronization refers to the synchronization of different media objects. Figure 2 represents an example of the temporal relationships in a multimedia application which begins with a video and audio sequence, and is synchronized with still images. Several techniques have been proposed based on the establishment of a global time [3, 10, 12], and using feedbacks [13, 14]. Hybrid systems based on the utilization of a global time and feedbacks have also been proposed [5]. These mechanisms will execute resynchronization actions to avoid

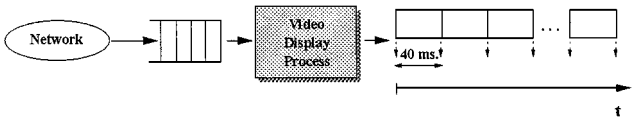

Figure 1. Intra-object synchronization.

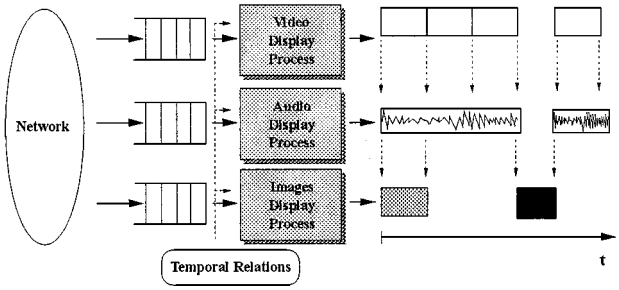

Figure 2. Inter-object synchronization.

asynchronies larger than certain thresholds, which are detectable by the user during playback [18].

With the aim of avoiding underflow and overflow, and therefore maintaining intra-object synchronization, it is necessary to analyze the amount of delay introduced by the network. Specifically, *delay* could be considered a measurement of the quality of service (QoS) in multimedia systems. In these systems there are two types of delay—latency and jitter. Latency is the delay between the generation of a signal—or retrieval from a storage system—and playback. Jitter is the dispersion of the delay between consecutive LDU's. The importance of delay depends on, the kind of the network (with or without QoS guarantee); the application; and the information objects involved. Real-time applications like video-conferencing require tight synchronization and small differences between capture; coding; storing; transmission; reception; and playback. This time interval is usually less than several tenths of a millisecond and the number of frames stored in the buffer is small, in order to minimize this delay. Nevertheless, in information retrieval systems, like video-on-demand, the main requirement is to reproduce the information at the same rate as the original capture rate. In this case, the difference between the capture and playback could be several seconds.

ATM networks which support multimedia services can use AAL-1 and AAL-5 levels to guarantee QoS with regard to, delay, jitter, and loss probability,—and so provide CBR and VBR services. Nevertheless, many current networks do not guarantee QoS, although in the near future they will, and users will be able to ask for a connection with a guaranteed QoS. Those connections with resource reservation will be more expensive than others. Some examples of networks without a QoS guarantee are: the Internet, which provides services known as "best-effort", without bandwidth, latency, jitter, error rate and throughput reservation; and also mobile networks—where there is no guarantee of available bandwidth while a user moves between cells (hand-off).

Audio is very sensitive to jitter, and the effect of random delays between consecutive LDU's is appreciable from the point of view of human perception. With video on the other hand, repetition and suppression of a small number of LDU's, and small random delays between consecutive frames, have little impact on human perception.

However, in real-time applications like in video-conferencing, the transmission rate can be highly variable—depending on the amount of movement and the quality of video. A transmission buffer is used reduce this variation. In information retrieval applications like video-on-demand, a constant transmission rate can be used because data is stored on disk. In the receiver, a high buffer occupation will point to a higher transmission than playback rate. A high playback rate could be caused by frames with a lot of motion video information, or a deviation in the normal playback rate of the decoder. On the other hand, a low occupation of the client buffer could be due to a slow transmission rate compared with the playback rate, or the existence of network congestion. In [6] *jitter rate* is defined for continuous objects like audio and video—as the time delay for original information playback caused by overflow and/or underflow. *Overflow jitter rate* is defined as the time interval during which data is lost because of overflow, and *underflow jitter rate* is defined in a similar way,—as the time interval during which no data is reproduced because of underflow. In the first scenario, the user would notice a skip in reproduction, and in the second, a pause in reproduction. Both effects will cause an asynchrony between audio and video, degrading the quality of the presentation.

To solve the problem of delay and jitter in networks without a QoS guarantee, multimedia clients *estimate the delay* and *control the buffer state* in order to maintain a continuous playback flow. Therefore, clients send feedback messages to the server, in order to adapt the transmission rate. To estimate delay mean and variance, a RTP/RTCP protocol [1], or a geometric and window estimator [4, 11], can be used. In [6], a feedback protocol is used for flow control and modification of the server transmission rate.

In figure 3, a complete flow control mechanism is described for applications based on the retrieval of stored information in networks with unguaranteed QoS, like video-on-demand. Once video information is captured, coded, and compressed, it is stored on disk, from where the transmitter process will retrieve and transmit it at a constant rate and specified quality. The transmission process could be considered as the most critical part of the system, because the flow control mechanism will work over the transmission rate. The reception buffer in the client peer should, in an ideal scenario, receive the data at a similar rate to transmission, perhaps with an added delay and a random variation (jitter) due to the effects of the network. Transmission and reception rates could be identical if resource reservation and congestion control mechanisms are used on the network. This is not the case for networks without a guaranteed QoS. Finally, the client plays back the frames with the aim of maintaining intra-frame synchronization.

The flow control mechanism is based on the utilization of the reception buffer state in order to modify the transmission rate. This feedbackward flow control scheme has several advantages over a feedforward scheme [6]. One of the principal advantages of using a feedback mechanism is that the information used for controlling the flow reflects with a great deal of precision the quality of the service being received by the client. This is because the client knows the exact state of the network and playback process without

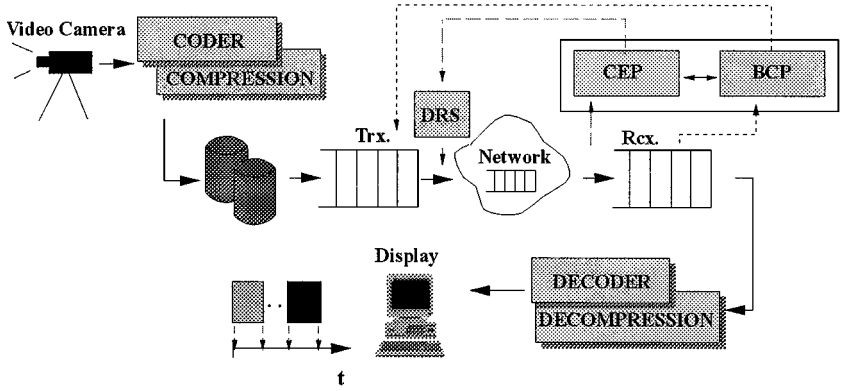

Figure 3. Generic diagram of flow control and congestion.

having to make any assumptions. Feedback control is based on the modification of the rates of transmission. The existing buffer state is detected by the Buffer Control Process (BCP). A high occupation of the client buffer will cause the client to send a feedback message to the server in order to reduce the transmission rate. Also, a low buffer occupation will result in a feedback message requesting an increase in the transmission rate. Nevertheless, it should be remembered that a low buffer occupation could be due to network congestion, and an increase of the transmission rate would be detrimental. A Congestion Estimation Process (CEP) can be used to detect the existence of congestion. If congestion is detected, the same feedback mechanism could be used but, instead of asking for an increase in the transmission rate, the client could request—via the Dynamic Rate Shaping (DRS)—a decrease in the quality of the images (possibly suppressing the high frequency components) [7], while maintaining the transmission rate.

In summary, three possibilities exist when using the CEP and BCP processes:

(a) Detection of a high occupation of the reception buffer. In this situation, the server is requested to reduce the transmission rate.
(b) Detection of a low occupation in the reception buffer, and the absence of congestion. The client requests an increase in the transmission rate.
(c) Detection of a low occupation of the reception buffer and the existence of congestion. The client requests a decrease in the quality of the kind of information (audio, video or fixed images), but maintains the transmission rate in frames per second. For instance, when embedded coding techniques are used, bits dropping mechanism could be implemented.

In this paper we focus on the analysis and evaluation of the BCP process which controls the flow control mechanism and the state of the client buffer.

The paper is organized as follows. In the second section, we explain qualitatively our proposal for a flow control mechanism. In the third section, the flow control is formulated

in terms of Markovian tools. The steady state probabilities are derived. The signaling traffic, for adjusting the server transmission rate, and its transmission rate dispersion are formulated in terms of steady state probabilities. The sojourn times operating at different transmission rates are also derived. The analysis shows the trade-off between signaling traffic and transmission rate dispersion. In Section 4 we show an illustrative example. Section 5 validates the analytical model by comparing it with the results of a real scenario. The paper ends with conclusions in Section 6.

2. Flow control mechanism

The proposed flow control mechanism to control the buffer state operates as follows (figure 4). Assuming that the client buffer is initially empty, the client begins to receive frames at a high rate λ_h. When the number of frames reaches the threshold L2, the client triggers a message towards the server requesting a lower transmission rate, say λ_m. The strategy is repeated if the buffer occupancy reaches another threshold L4, i.e., the client requests a new reduction in the transmission rate, say from λ_m to λ_l. In the opposite way, the client will order the server to increase the transmission rate when buffer occupancy is reduced. However, due to fluctuations in buffer occupancy, a "ping-pong" effect can happen. That is, the "up" and "down" switching in the transmission rate can produce an overload in the signaling control traffic. To mitigate this phenomenon, two pairs of thresholds (L1, L2), (L3, L4) are chosen, so that ($0 < \mathrm{L1} < \mathrm{L2} < \mathrm{L3} < \mathrm{L4} < \mathrm{N}$). As explained before, if the upward transitions $\mathrm{L2}-1->\mathrm{L2}$ and $\mathrm{L4}-1->\mathrm{L4}$ produce respectively a change in the transmission rate $\lambda_h -> \lambda_m$ and $\lambda_m -> \lambda_l$, then the downward transitions $\mathrm{L1} < -\mathrm{L1}+1$ and $\mathrm{L3} < -\mathrm{L3}+1$ will produce the changes $\lambda_h < -\lambda_m$ and $\lambda_m < -\lambda_l$ respectively.

3. Analytical formulation

The Poisson frame arrival process is assumed for each client. The rate is state dependent on the client buffer occupancy. The consumption frame rate is assumed to be exponentially distributed. Using the input Poisson process and exponential distributions simplify the analysis because of the inherent memorylessness. In real applications, the traffic could be considered as periodically generated, and subject to a normal distribution delay when traveling through a network. And finally, consumption—with a given playback rate—could also be considered periodic. However, section 5 shows that the model captures the behavior of a real system, and therefore validates our Markovian model.

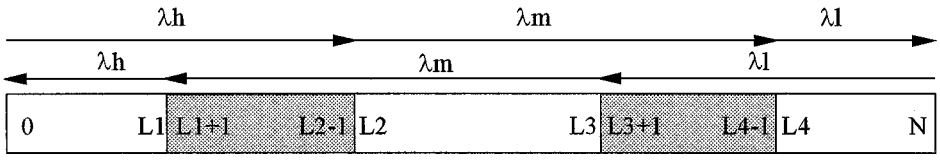

Figure 4. Flow control mechanism and buffer occupancy.

Table 1. Table of symbols.

$\lambda_h, \lambda_m, \lambda_l$	Birth rates: *high*, *medium* and *low*. (*LDU's/s.*)
μ	Client consumption rate. (*LDU's/s.*)
L1, L2, L3, L4	Client buffer thresholds.
q_i, p_i, r_i	Steady state probabilities.
$\alpha = \frac{\mu}{\lambda_h}; \gamma = \frac{\lambda_m}{\mu}; \beta = \frac{\lambda_l}{\mu}$	Relationship between rates.
$\phi_{hm}, \phi_{mh}, \phi_{lm}, \phi_{ml}$	Change request rate over the transmission rate. (*switching/s.*)
$T_{hm}, T_{mh}, T_{lm}, T_{ml}$	Expected time between requests. (*s./switching*)
P_h, P_m, P_l	Percentage of time working at *high*, *medium* and *low* rates.
$ST_{hm}(ST_{mh})$	Mean residence time at (*no*) *high* rate. (*s.*).
$T_{hm} = ST_{mh} + ST_{hm}$	
$ST_{lm}(ST_{ml})$	Mean residence time at (*no*) *low* rate. (*s.*).
$T_{lm} = ST_{ml} + ST_{lm}$	

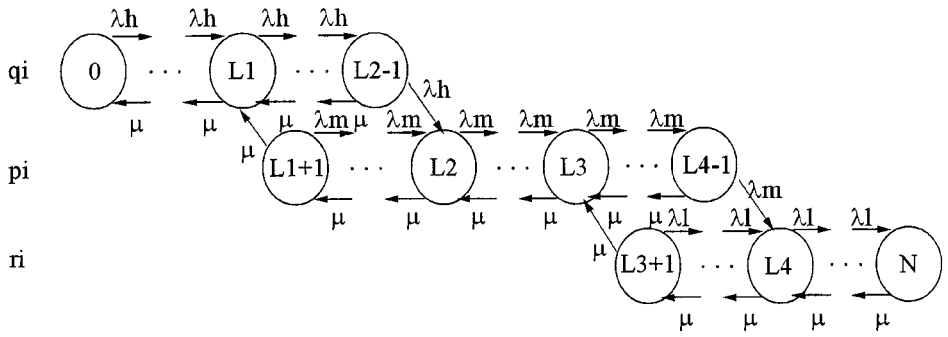

Figure 5. Markov process of the flow control model.

The system is characterized by a birth-death process. N is the client buffer capacity, expressed in frames. Three birth rates are considered, *high* (λ_h), *medium* (λ_m) and *low* (λ_l); and a consumption rate (μ). *Medium* rate is the nominal rate (Table 1).

The study of the flow control mechanism starts from the general scenario of two hysteresial areas, similar to [2]. Note that a scenario without hysteresis (L1 = L2 −1 and L3 = L4 −1), and a scenario with maximum hysteresis (L2 = L3), considered in [6], are obtained from our general study. Figure 5 shows the corresponding Markov process.

3.1. Steady state probabilities

Using the same methodology as [8], the **steady state probabilities** q_i, p_i, and r_i are obtained, and then used for calculating those parameters (in Sections 3.1, 3.2, 3.3 and 3.4) which allow us to evaluate the control mechanism. Choosing appropriates cuts (figure 6) we write the corresponding flow equations:

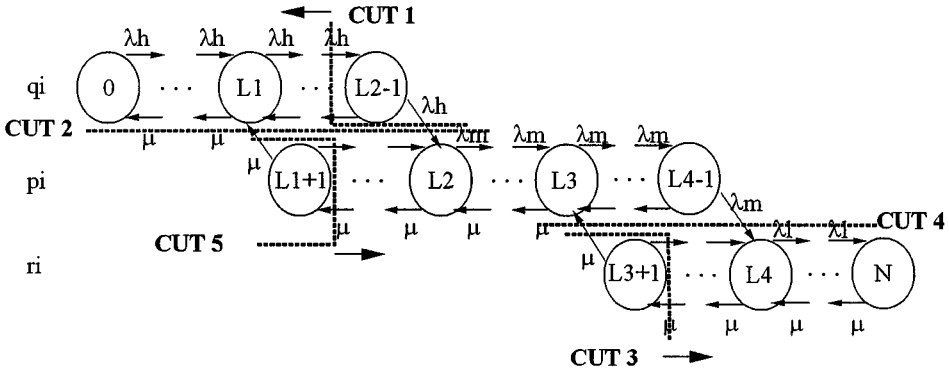

Figure 6. Cuts for the flow control equations calculus.

CUT 1:

$$\lambda_h \cdot q_{L2-2} = \mu \cdot q_{L2-1} + \lambda_h \cdot q_{L2-1} \qquad (1.L2-2)$$
$$\lambda_h \cdot q_{L2-3} = \mu \cdot q_{L2-2} + \lambda_h \cdot q_{L2-1} \qquad (1.L2-3)$$
$$\lambda_h \cdot q_{L2-4} = \mu \cdot q_{L2-3} + \lambda_h \cdot q_{L2-1} \qquad (1.L2-4)$$
$$\lambda_h \cdot q_{L1} = \mu \cdot q_{L1+1} + \lambda_h \cdot q_{L2-1} \qquad (1.L1)$$
$$\lambda_h \cdot q_{L1-1} + \mu \cdot p_{L1+1} = \mu \cdot q_{L1} + \lambda_h \cdot q_{L2-1} \qquad (1.L1-1)$$
$$\lambda_h \cdot q_{L1-2} + \mu \cdot p_{L1+1} = \mu \cdot q_{L1-1} + \lambda_h \cdot q_{L2-1} \qquad (1.L1-2)$$
$$\vdots$$
$$\lambda_h \cdot q_0 + \mu \cdot p_{L1+1} = \mu \cdot q_1 + \lambda_h \cdot q_{L2-1} \qquad (1.0)$$

CUT 2:

$$\lambda_h \cdot q_{L2-1} = \mu \cdot p_{L1+1} \qquad (2.L2-1)$$

CUT 3:

$$\mu \cdot r_{L3+2} = \lambda_l \cdot r_{L3+1} + \mu \cdot r_{L3+1} \qquad (3.L3+2)$$
$$\mu \cdot r_{L3+3} = \lambda_l \cdot r_{L3+2} + \mu \cdot r_{L3+1} \qquad (3.L3+3)$$
$$\mu \cdot r_{L3+4} = \lambda_l \cdot r_{L3+3} + \mu \cdot r_{L3+1} \qquad (3.L3+4)$$
$$\vdots$$
$$\mu \cdot r_{L4} = \lambda_l \cdot r_{L4-1} + \mu \cdot r_{L3+1} \qquad (3.L4)$$
$$\mu \cdot r_{L4+1} + \lambda_m \cdot p_{l4-1} = \lambda_l \cdot r_{L4} + \mu \cdot r_{L3+1} \qquad (3.L4+1)$$
$$\mu \cdot r_{L4+2} + \lambda_m \cdot p_{l4-1} = \lambda_l \cdot r_{L4+1} + \mu \cdot r_{L3+1} \qquad (3.L4+2)$$
$$\vdots$$
$$\mu \cdot r_N + \lambda_m \cdot p_{l4-1} = \lambda_l \cdot r_{N-1} + \mu \cdot r_{L3+1} \qquad (3.N)$$

CUT 4:

$$\mu \cdot r_{L3+1} = \lambda_m \cdot p_{l4-1} \qquad (4.L3+1)$$

CUT 5:

$$\mu \cdot p_{L1+2} = \lambda_m \cdot p_{L1+1} + \mu \cdot p_{L1+1} \qquad (5.L1+2)$$
$$\mu \cdot p_{L1+3} = \lambda_m \cdot p_{L1+2} + \mu \cdot p_{L1+1} \qquad (5.L1+3)$$
$$\mu \cdot p_{L1+4} = \lambda_m \cdot p_{L1+3} + \mu \cdot p_{L1+1} \qquad (5.L1+4)$$
$$\vdots$$
$$\mu \cdot p_{L2} = \lambda_m \cdot p_{L2-1} + \mu \cdot p_{L1+1} \qquad (5.L2)$$
$$\mu \cdot p_{L2+1} + \lambda_h \cdot q_{L2-1} = \lambda_m \cdot p_{L2} + \mu \cdot p_{L1+1} \qquad (5.L2+1)$$
$$\mu \cdot p_{L2+2} + \lambda_h \cdot q_{L2-1} = \lambda_m \cdot q_{L2+1} + \mu \cdot p_{L1+1} \qquad (5.L2+2)$$
$$\vdots$$
$$\mu \cdot p_{L3} + \lambda_h \cdot q_{L2-1} = \lambda_m \cdot p_{L3-1} + \mu \cdot p_{L1+1} \qquad (5.L3)$$
$$\mu \cdot p_{L3+1} + \lambda_h \cdot q_{L2-1} + \mu \cdot r_{L3+1} = \lambda_m \cdot p_{L3} + \mu \cdot p_{L1+1} \qquad (5.L3+1)$$
$$\mu \cdot p_{L3+2} + \lambda_h \cdot q_{L2-1} + \mu \cdot r_{L3+1} = \lambda_m \cdot p_{L3+1} + \mu \cdot p_{L1+1} \qquad (5.L3+2)$$
$$\vdots$$
$$\mu \cdot p_{L4-1} + \lambda_h \cdot q_{L2-1} + \mu \cdot r_{L3+1} = \lambda_m \cdot p_{L4-2} + \mu \cdot p_{L1+1} \qquad (5.L4-1)$$

For simplicity, we will use the following notation:

$$\alpha = \frac{\mu}{\lambda_h}; \quad \gamma = \frac{\lambda_m}{\mu}; \quad \beta = \frac{\lambda_l}{\mu}$$

It is desirable that the system works at nominal rate λ_m as much of the time as possible. Therefore, it is reasonable to assume $\alpha < 1$ and $\beta < 1$, since those values force the system to reside in states p_i, for long periods of time. This parameter choice avoids high probability of underflow ($\alpha < 1$) and overflow ($\beta < 1$). The value of λ_m is chosen to coincide with the nominal consumption rate μ, and therefore $\gamma = 1$.

To obtain the set of probabilities q_i, r_i and p_i, we first insert the Eq. $(1.L2-2)$ in the Eq. $(1.L2-3)$ to express the value q_{L2-3} as a function of q_{L2-1}. In the same way, we insert the Eq. $(1.L2-3)$ in the Eq. $(1.L2-4)$ to obtain the value of q_{L2-4} in terms of q_{L2-1}. By repeating this process and using the equations of Cut 2 $(2.L2-1)$ we obtain the following expressions for q_i:

$$\begin{aligned} q_i &= \left(\frac{1-\alpha^{L2-i}}{1-\alpha}\right) \cdot q_{L2-1} - \left(\frac{1-\alpha^{L1-i}}{1-\alpha}\right) \cdot \alpha \cdot p_{L1+1} \\ &= \left(\frac{\alpha^{L1-i} - \alpha^{L2-i}}{1-\alpha}\right) \cdot \alpha \cdot p_{L1+1}, \quad i = 0, 1, \ldots, L1-1 \end{aligned} \qquad (1)$$

$$q_i = \left(\frac{1-\alpha^{L2-i}}{1-\alpha}\right)\cdot q_{L2-1} = \left(\frac{1-\alpha^{L2-i}}{1-\alpha}\right)\cdot \alpha \cdot p_{L1+1},$$
$$i = L1, L1+1, \ldots, L2-1 \tag{2}$$

By adding these equations and applying some simple algebra operations we get the following expression:

$$\sum_{i=0}^{L2-1} q_i = q_{L2-1}\cdot\left(\frac{(1-\alpha)\cdot(L2-L1)+\alpha^{L2+1}-\alpha^{L1+1}}{(1-\alpha)^2}\right)$$
$$= \alpha \cdot p_{L1+1}\left(\frac{(1-\alpha)\cdot(L2-L1)+\alpha^{L2+1}-\alpha^{L1+1}}{(1-\alpha)^2}\right) \tag{3}$$

Following a similar process, and using the expressions of Cut 3 and Cut 4, we obtain the following equations for the probabilities of r_i:

$$r_i = \left(\frac{1-\beta^{i-L3}}{1-\beta}\right)\cdot r_{L3+1} = \left(\frac{1-\beta^{i-L3}}{1-\beta}\right)\cdot\gamma\cdot p_{L4-1}, \quad i = L3+1,\ldots,L4 \tag{4}$$
$$r_i = \left(\frac{1-\beta^{i-L3}}{1-\beta}\right)\cdot r_{L3+1} - \left(\frac{1-\beta^{i-L4}}{1-\beta}\right)\cdot\gamma\cdot p_{L4-1}$$
$$= \left(\frac{\beta^{i-L4}-\beta^{i-L3}}{1-\beta}\right)\cdot\gamma\cdot P_{L4-1}, \quad i = L4,\ldots,N \tag{5}$$

The sum of the Eqs. (4) and (5) can be expressed as:

$$\sum_{i=L3+1}^{N} r_i = r_{L3+1}\cdot\left(\frac{(1-\beta)\cdot(L4-L3)+\beta^{N-L3+1}-\beta^{N-L4+1}}{(1-\beta)^2}\right)$$
$$= \gamma\cdot P_{L4+1}\left(\frac{(1-\beta)\cdot(L4-L3)+\beta^{N-L3+1}-\beta^{N-L4+1}}{(1-\beta)^2}\right) \tag{6}$$

Finally, with the flow equations of the p_i probabilities and using Cut 5, Cut 2 and Cut 4, we obtain the general equations for the probabilities of p.

$$p_i = \left(\frac{1+\gamma^{i-L1}}{1+\gamma}\right)\cdot p_{L1+1}, i = L1+1,\ldots,L2 \tag{7}$$
$$p_i = \left(\frac{1+\gamma^{i-L1}}{1+\gamma}\right)\cdot p_{L1+1} - \left(\frac{1+\gamma^{i-L2}}{1+\gamma}\right)\cdot\frac{1}{\alpha}\cdot q_{L2-1}$$
$$= \left(\frac{\gamma^{i-L1}-\gamma^{i-L2}}{1+\gamma}\right)\cdot p_{L1+1}, \quad i = L2+1,\ldots,L3 \tag{8}$$
$$p_i = \left(\frac{1+\gamma^{i-L1}}{1+\gamma}\right)\cdot p_{L1+1} - \left(\frac{1+\gamma^{i-L2}}{1+\gamma}\right)\cdot\frac{1}{\alpha}\cdot q_{L2-1} - \left(\frac{1+\gamma^{i-L3}}{1+\gamma}\right)\cdot r_{L3+1}$$

$$= \left(\frac{\gamma^{i-L1} - \gamma^{i-L2}}{1+\gamma}\right) \cdot p_{L1+1} - \left(\frac{1+\gamma^{i-L3}}{1+\gamma}\right) \cdot, \gamma \cdot p_{L4-1},$$
$$i = L3+1, \ldots, L4-1 \tag{9}$$

By adding Eqs. (7), (8) and (9), we get the following equation—which represents the sum of the p_i probabilities.

$$\sum_{i=L1+1}^{L4-1} p_i = p_{L1+1} \cdot \left(\frac{(1-\gamma)\cdot(L2-L1) + \gamma^{L4-L1} - \gamma^{L4L2}}{(1-\gamma)^2}\right) - \gamma \cdot p_{L4-1}\left(\frac{(1-\gamma)\cdot(L4-L3-1) + \gamma^{L4-L3} - \gamma}{(1-\gamma)^2}\right) \tag{10}$$

Taking into account that the following equation has to be completed:

$$\sum_{i=0}^{L2-1} q_i + \sum_{i=L1+1}^{L4-1} p_i + \sum_{i=L3+1}^{N} r_i = 1 \tag{11}$$

and substituting each summary in the previous equation for the expressions shown in (3), (6) and (10), we obtain the first equation of our system.

$$p_{L1+1}\left(\alpha \cdot \frac{(1-\alpha)\cdot(L2-L1) + \alpha^{L2+1} - \alpha^{L1+1}}{(1-\alpha)^2} + \frac{(1-\gamma)\cdot(L2-L1) + \gamma^{L4-L1} - \gamma^{L4+L2}}{(1-\gamma)^2}\right) + \gamma \cdot p_{L4-1}\left(\frac{(1-\beta)\cdot(L4-L3) + \beta^{N-L3+1} - \beta^{N-L4+1}}{(1-\beta)^2} - \frac{(1-\gamma)\cdot(L4-L3-1) - \gamma + \gamma^{L4-L3}}{(1-\gamma)^2}\right) = 1 \tag{12}$$

The second equation can be obtained from the p_{L4-1} probability obtained in expression (9). From this equation, and using the equations of Cut 2 (Eq. $(2.L2-1)$) and Cut 4 (Eq. $(4.L3+1)$), we get the following:

$$p_{L4-1}(1-\gamma^{L4-L3}) = p_{L1+1}(\gamma^{L4-L2-1} - \gamma^{L4-L1-1}) \tag{13}$$

By solving the lineal Eqs. (12) and (13) we obtain and p_{L1+1} and p_{L4-1}. By successively substituting the Eqs. (1), (2), (4), (5), (8) and (9), we obtain all of the state probabilities q_i, r_i and p_i which are needed to calculate the parameters of the flow control mechanism.

3.2. *Signaling traffic*

Change request rate over the transmission rate can be calculated from the previous state probabilities. The change rate from *high* to *medium*, coinciding with rate change from *medium* to *high*, is given by:

$$\phi_{hm} = \phi_{mh} = q_{L2-1} \cdot \lambda_h = p_{L1+1} \cdot \mu \tag{14}$$

Similarly, the change rate from *low* to *medium*, coinciding from *medium* to *low*, is given by:

$$\phi_{ml} = \phi_{lm} = p_{L4-1} \cdot \lambda_m = r_{L3+1} \cdot \mu \tag{15}$$

Equivalently, the expected time between requests, for rate changes from *high* to *medium* (or from *medium* to *high*) and from *medium* to *low* (or from *low* to *medium*), is given by:

$$T_{hm} = T_{mh} = 1/\phi_{hm} = 1/\phi_{mh} = 1/(q_{L2-1} \cdot \lambda_h) = 1/(p_{L1+1} \cdot \mu) \tag{16}$$

$$T_{ml} = T_{lm} = 1/\phi_{ml} = 1/\phi_{lm} = 1/(p_{L4-1} \cdot \lambda_m) = 1/(r_{L3+1} \cdot \mu) \tag{17}$$

3.3. *Transmission rate dispersion*

We consider λ_m as nominal transmission rate. The server simultaneously attends a total of M number of users, which are statistically independent. It is desirable to operate with a minimum dispersion from the nominal transmission rate. The probability that M_h clients receive data with a *high* rate, M_m with a *medium* rate and M_l with a *low* rate ($M_h + M_m + M_l = M$), is:

$$P(M_h, M_m, M_l) = \frac{M!}{M_h! M_m! M_l!} P_h^{M_h} \cdot P_m^{M_m} \cdot P_l^{M_l} \tag{18}$$

P_h, P_m, P_l are respectively the probabilities, or time pecentages, of working at *high*, *medium* and *low* rates. They are given by $P_h = \sum_i q_i$, $P_m = \sum_i p_i$ and $P_i = \sum_i r_i$. Obviously, the difference between the number of clients working with *low* and *high* rates should be $Z = |M_h - M_l| \leq z$, as shown by figure 7. We will denote the probability of this event as $\Pr(Z \leq z)$.

Bearing in mind figures 5 and 7, and for a fixed value z, we see that $\Pr(Z \leq z)$ (Eq. (19)) is smaller because the hysteresial areas are smaller. However, large hysteresial areas are needed to reduce flow control signaling traffic. This trade-off is analyzed with illustrative examples in Section 4.

$$\Pr(Z \leq z) = \sum_{\substack{M_h + M_m + M_l = M \\ |M_h - M_l| \leq z}} P(M_h, M_m, M_l) \tag{19}$$

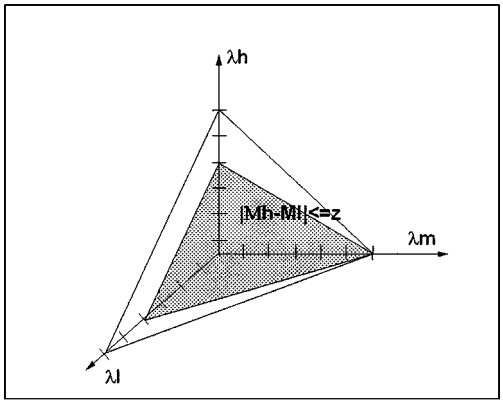

Figure 7. Tridimensional plan of the condition $Z = |M_h - M_l| \leq z$.

3.4. Sojourn times

Similarly to [6], another interesting parameter is the expected time of residence in each of the transmission rates, *high*, *medium* and *low*. For example, the time elapsed between transitions (L1 $+1->$L1) and (L2 $-1->$L2) (figure 8), can be calculated recursively using [2]:

$$ST_{hm} = \overline{r_{c,L1}(0, L2-1)} = \sum_{n=L1}^{j} \overline{r_{c,o}(i,n)} \tag{20}$$

where,

$$\overline{r_{c,o}(i,j)} = \frac{1+\mu_j \cdot \overline{r_{c,o}(i,j-1)}}{\lambda_j}; \quad j = i, i+1, i+2, \ldots$$
$$\overline{r_{c,o}(i,i-1)} = 0 \tag{21}$$

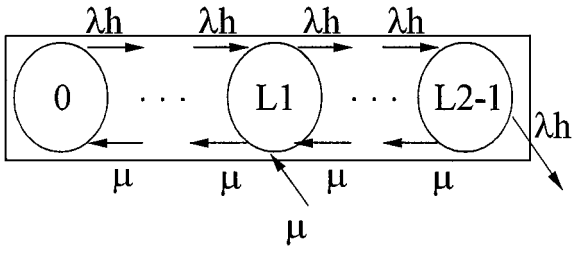

Figure 8. Permanence states in high rate.

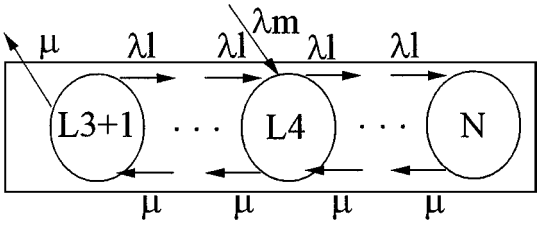

Figure 9. Permanence states in low rate.

Similarly, the expected time between transitions (L4 $-1-$ >L4) and (L3 $+1-$ >L3) (figure 9) can be calculated according to:

$$ST_{lm} = \overline{r_{L4,c}(L3+1, N)} = \sum_{n=L4}^{L3+1} \overline{r_{o,c}(n, N)} \tag{22}$$

where,

$$\begin{aligned} \overline{r_{o,c}(i, j)} &= \frac{1 + \lambda_i . \overline{r_{o,c}(i+1, j)}}{\mu_i}; \quad i = j, j-1, j-2, \ldots \\ \overline{r_{o,c}(j+1, j)} &= 0 \end{aligned} \tag{23}$$

Let ST_{mh} be the expected time from when the L2 state is reached until the transition between L1 + 1 − >L1 is executed (figure 10). This can be obtained by the observation of a cycle (referred to *high* rate) of the regenerative process [15] shown in figure 11.

With the expected cycle time (T_{hm}) and ST_{hm}, the expression of ST_{mh} is represented by:

$$ST_{mh} = T_{hm} - ST_{hm} \tag{24}$$

ST_{ml} is denoted as the expected time from when the L3 state is reached until the transition between L4 $-1-$ >L4 is executed (figure 12). This can be obtained using similar arguments to the calculation of ST_{mh}.

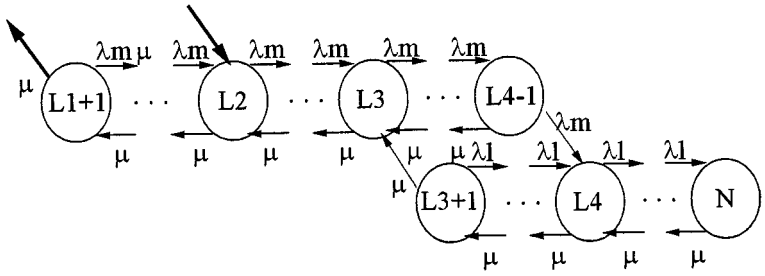

Figure 10. Permanence states out of high rate.

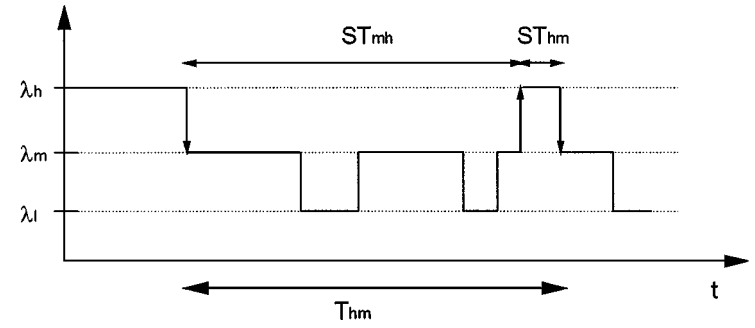

Figure 11. Cycle of the regenerative process refereed to high rate.

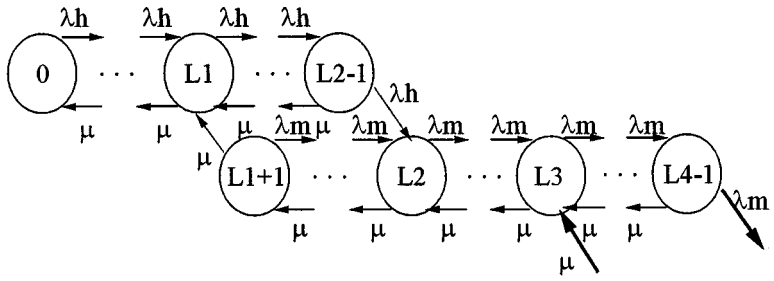

Figure 12. Permanence states out of low rate.

With the expression of T_{lm} calculated by using Eq. (14) and ST_{lm}, then ST_{ml} is represented by:

$$ST_{ml} = T_{lm} - ST_{lm} \tag{25}$$

3.5. *Thresholds selection*

Looking at the figure 5 state transition diagram, we intuitively observe that the "underflow" (E_0) state probability is strongly controlled by the L1 threshold. This is due to its proximity to state E_0 and to the choice $\gamma = 1$. Therefore, this probability can be reduced by choosing $\alpha < 1$. A similar observation can be made with respect to the "overflow" (E_N) state and the L4 threshold. The choice of $\beta < 1$ is therefore recommended. Some refined procedures could be used to choose L1 and L4. However, at first glance, the values proposed in [6], L1 $= 0.1^*N$, and L4 $= 0.9^*N$, are chosen. The selection of L2 and L3 thresholds are made according to the following criteria:

(c1) For an arbitrating client—to limit the mean number of requests per time unit for changes of transmission rate.
(c2) Limit the probability $\Pr(Z \leq z)$ to a given fixed value.

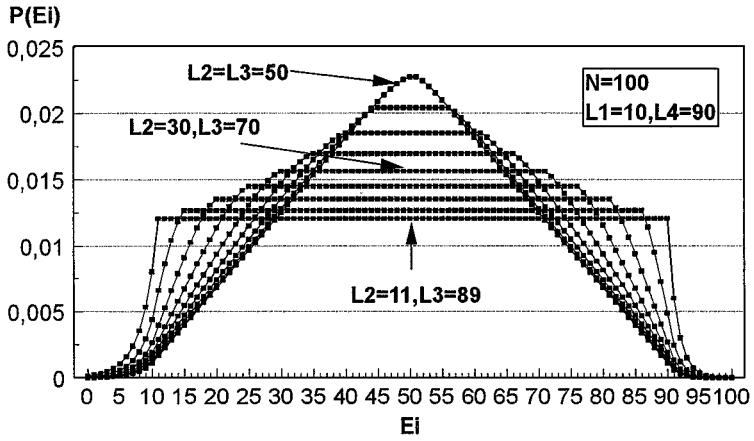

Figure 13. State probabilities Pi.

4. Illustrative example

As in [6] we have chosen a buffer size of $N = 100$ for each client, and a transmission rate of $\lambda_m = \mu$, $\lambda_h = 1.5 \cdot \lambda_m$, $\lambda_l = 0.5 \cdot \lambda_m (\alpha = 2/3, \gamma = 1, \beta = 1/2)$. The state probabilities $P_i = q_i + p_i + r_i$, $\forall i$, are shown in figure 13.

As expected, the probabilities P_i for $i < L1$ and $i > L4$ are very small, which implies that the "underflow" and "overflow" probabilities of P_0 and P_N, are strongly controlled by the thresholds L1 and L4 respectively, as well as the α and β parameters. We also observe the tendency for a major percentage of probability to concentrate in the central zone as the hysteresial areas increase, i.e., as the distance $L2 - L1 + L4 - L3$ increases. In the scenario of no hysteresis ($L2 = L1 + 1 = 11$ and $L3 = L4 - 1 = 89$), the state probabilities are more uniformly distributed. As the size of the hysteresial areas increase, for example ($L2 = 30$, $L3 = 70$), the central state probabilities increase, with the most extreme situation occurring when $L2 = L3$ ($L2 = L3 = 50$).

On the order hand, figures 14 and 15 show the mean number of changes per second from *high* to *medium*, and from *medium* to *low*. Both plots coincide, because of the symmetry of the threshold ($L2 - L1 = L4 - L3$) and rate selection ($\lambda_m = \mu$, $\lambda_h = 1.5 \cdot \lambda_m$, $\lambda_l = 0.5 \cdot \lambda_m$). In both plots, the efficiency of using hysteresial techniques for flow control can be seen. Without hysteresis ($L2 = L1 + 1 = 11$, $L3 = L4 - 1 = 89$), request messages are issued by the client at a rate of 0.3 per second. But with values $L2 = 15$, $L3 = 85$, the rate is reduced to the sixth part, and with a less appreciable reduction for larger hysteresial distances. For the limit values of $L2 = L3 = 50$, the rate change reaches a minimum of 0.014 switchings per second.

Let $l = L4 - L3 + L2 - L1$ be the distance of the hysteresial area. Figure 16 represents the rate change for every possible configuration, in terms of l. We observe that the symmetric configuration ($L4 - L3 = L2 - L1$) reflects the minimum rate of changes. Figure 17 shows the envelope of figure 16 for the symmetric scenario.

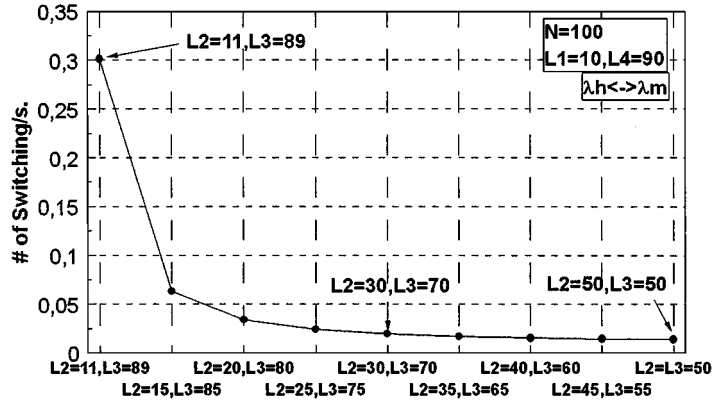

Figure 14. Rate change from high to medium and vice versa.

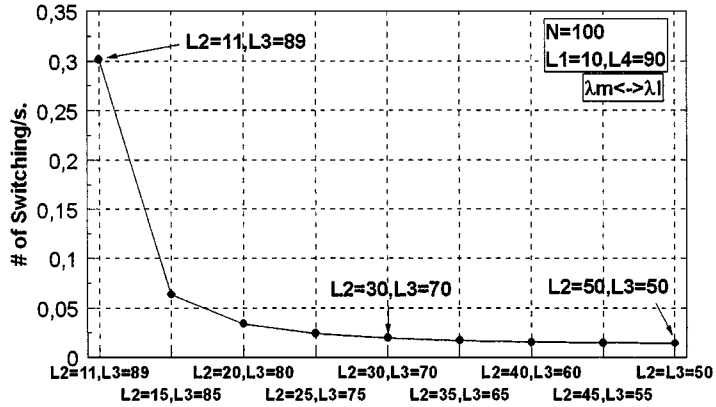

Figure 15. Rate change from low to medium and vice versa.

The advantages of using hysteresial techniques can be also appreciated if the expected time between changes is observed. Figures 18 and 19, similar to figures 14 and 15, represent the time expected between requests for different values of L2 and L3. Figure 20 represents the mean time between requests for every possible combination, and figure 21 shows the best cases, i.e., the symmetric configurations (L2 − L1 = L4 − L3). It can be observed that while clients without hysteresis signal each 3.33 seconds, those clients with hysteresis implemented at L2 = L3 = 50, signal each 71.42 seconds. This proves the tremendous effectiveness of the hysteresial mechanism.

Figure 22 shows the values ST_{mh}, ST_{hm}, ST_{ml}, ST_{lm} for different configurations. Those values give us an idea of the time elapsed from when a rate is reached until it changes. It can be observed that as the hysteresial area increases, the residence time in *high* (ST_{hm}) and *low* (ST_{lm}) rates slowly increases. On the other hand, the residence time at *medium* rate increases considerably with the hysteresial distance.

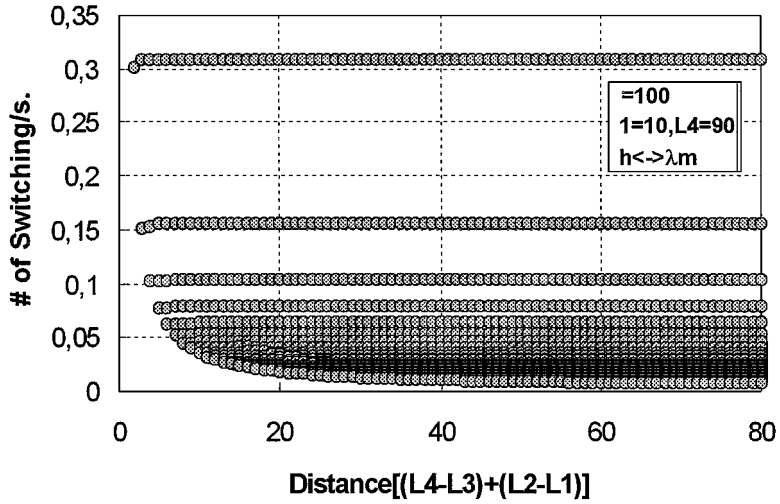

Figure 16. Number of switchings depending on the hysteretic distance $d = \mathrm{L4} - \mathrm{L3} + \mathrm{L2} - \mathrm{L1}$.

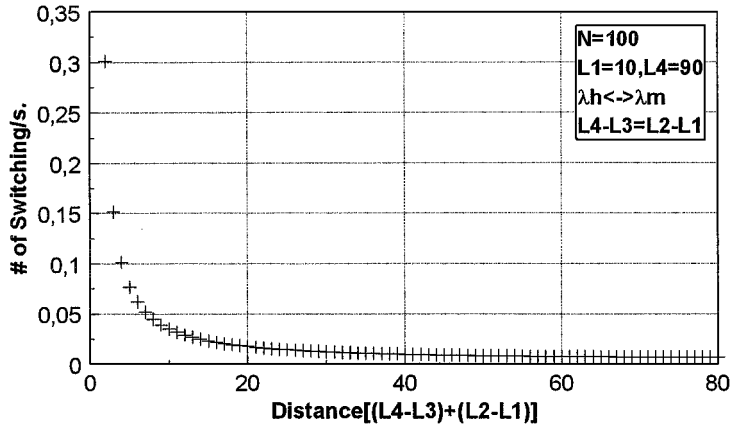

Figure 17. Envelope of the values in figure 16.

Figure 23 plots the percentage of time during which the server transmits at *high*, *medium* and *low* rates for each client. We observe that, as the hysteresial area decreases, the probability of the server transmitting at medium rate (nominal) increases. The best case is when there is no hysteresis ($\mathrm{L2} = \mathrm{L1} + 1 = 11$, $\mathrm{L3} = \mathrm{L4} - 1 = 89$). Figure 24 shows the time elapsed by the server operating at each rate, in terms of buffer size N, choosing as thresholds $\mathrm{L1} = 0.1^{*}N$, $\mathrm{L2} = 0.3^{*}N$, $\mathrm{L3} = 0.7^{*}N$ y $\mathrm{L4} = 0.9^{*}N$, and where the buffer size changes from 1 second ($N = 25$) to 10 seconds ($N = 250$). This demonstrates that as the buffer size increases, the probability of finding the server transmitting at a *medium* rate

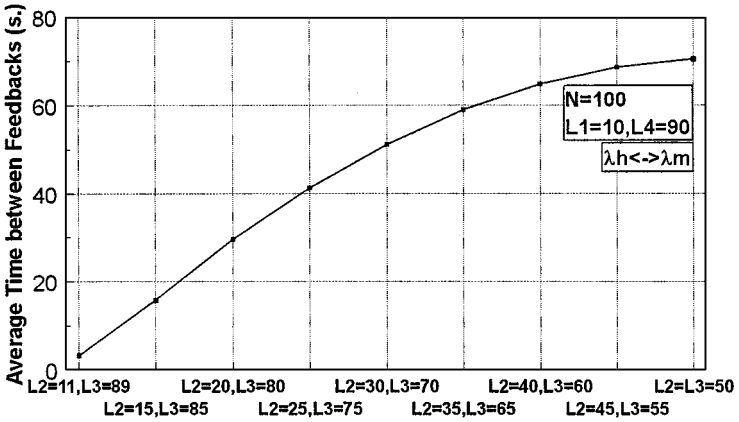

Figure 18. Mean time between changes from high to medium rates and vice versa.

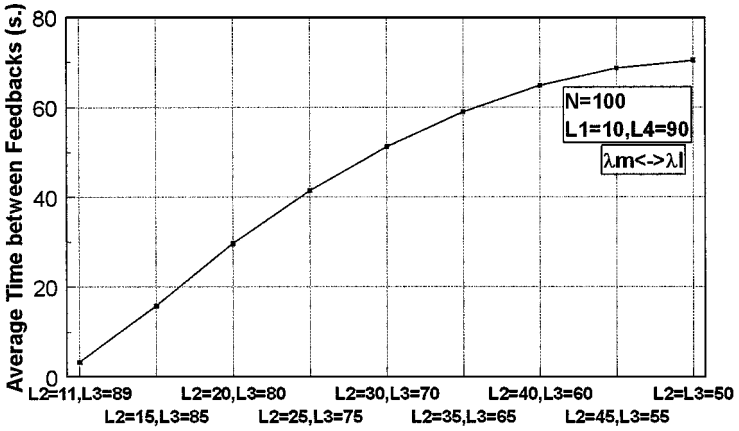

Figure 19. Mean time between changes from low to medium rates and vice versa.

also increases, and the probability of finding it transmitting at *low* or *high* rates decreases. Finally, for $M = 10$ clients, figure 25 represents the probability of $|M_h - M_l| \leq 3$. Results provide a general view of the effect of hysteresis over this second criterion (c2 Section 3.4)

If only the first criteria were used, (c1 Section 3.4), we would require that L2 = L3 = 50—a proposal which coincides with [6]. Nevertheless, this selection coincides with a minimal probability of non-dispersion $\Pr(Z \leq z)$. To maximize this, we must select a scenario with L2 = L1 + 1 and L3 = L4 − 1, as this would provide a maximized switching rate. It can be seen that with a small increase (decrease) of L2 (L3), an excellent compromise between the two considered criteria is achieved—as the knee of figures 14 and 15 shows. For example, with L2 = 15 and L3 = 85, the number of rate changes decreases to the sixth part of the maximum value, while the non-dispersion probability $\Pr(Z \leq z)$ is reduced by only approximately 5%.

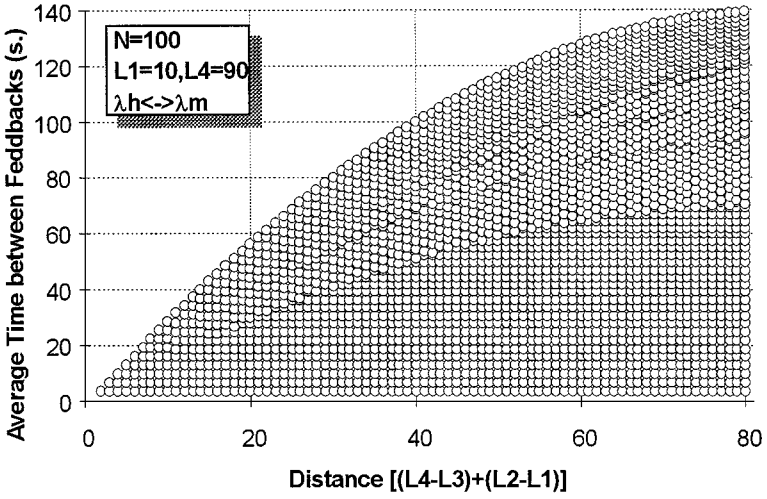

Figure 20. Mean time between changes depending on the hysteretic distance $l = \mathrm{L4} - \mathrm{L3} + \mathrm{L2} - \mathrm{L1}$.

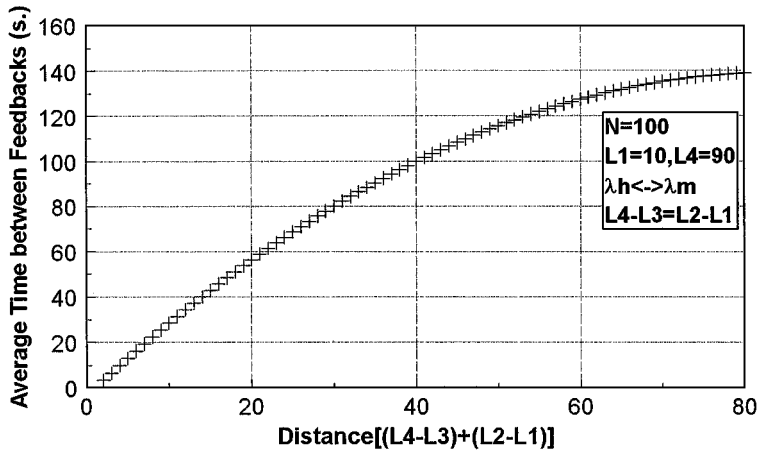

Figure 21. Envelope of the values in figure 20.

5. Model validation

In the previous section the performance results, using the hysteresis technique, were presented. These results verify that the signalling reduction effect is satisfactory and valid to implement flow control in a completely generic environment. With the aim of testing the results in a real scenario, we have developed a multimedia application for video distribution over Internet. This application is integrated in the WWW, and has been designed to guarantee multimedia signaling and flow control. The application has been developed using ActiveX and DirectShow API tool.

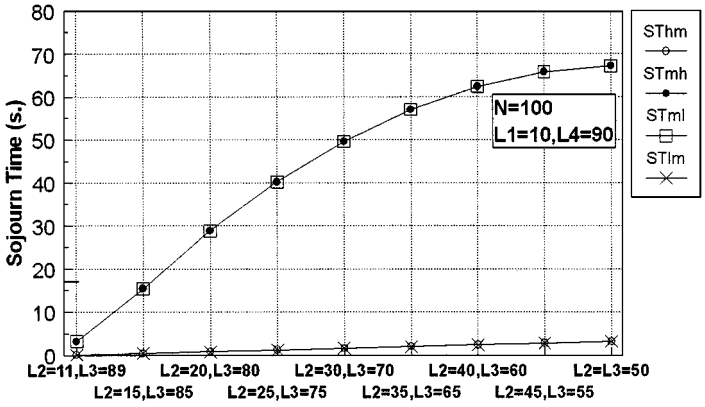

Figure 22. Permanence mean times.

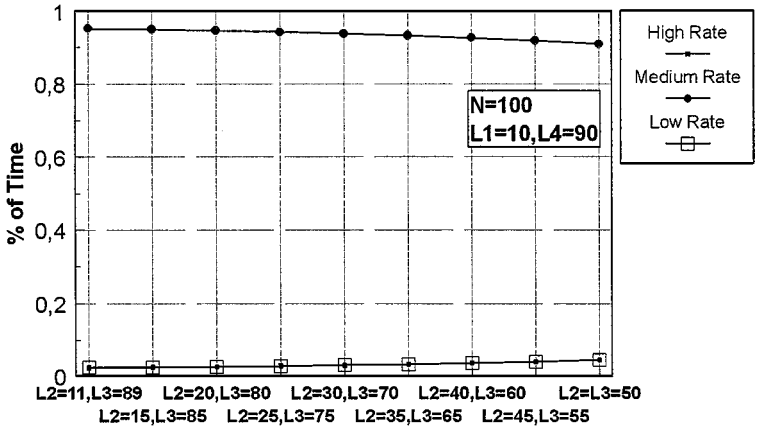

Figure 23. Percentage of time in low, medium and high rates.

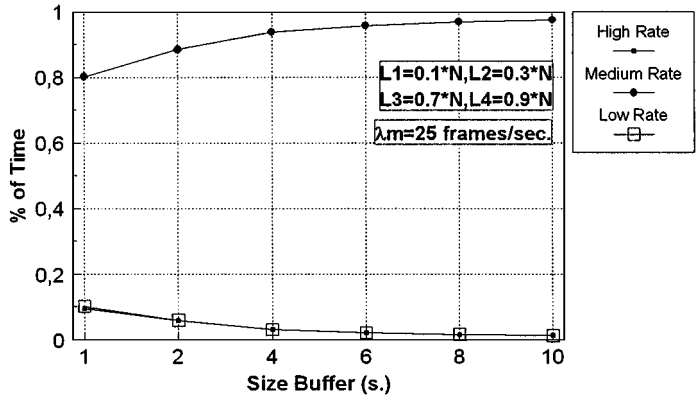

Figure 24. Percentage of time in low, medium and high rates depending on N.

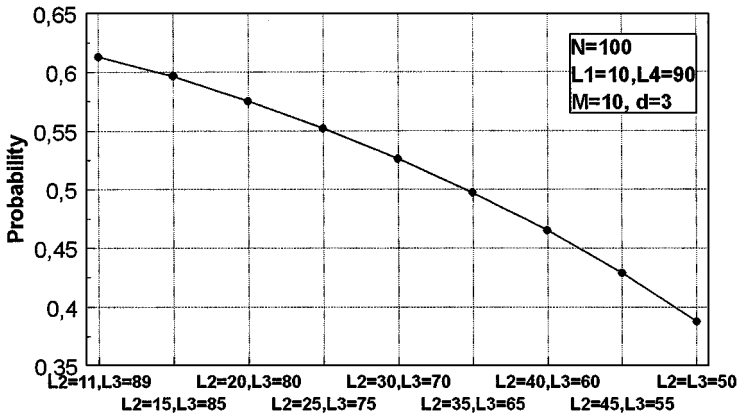

Figure 25. No dispersion probabilities.

In figure 26 are shown the architecture and elements which compose the system. The main parts of the system are the multimedia server and the client stations. The multimedia server is in charge of storing the information (video, text, audio, etc.) which will be playback lately by the client stations. A WWW server was used as multimedia server, running on a Sun Sparc workstation. The multimedia files were stored using the MPEG and AVI compression formats. The access to the files is achieved by a single request to an URL address, which makes reference to the multimedia server. From the point of view of the playback all the client stations add the same ActiveX control, which provide the typical playback and visualization options (play, stop, forward, reverse, pause, etc.). Nevertheless, from the flow control point of view, it is possible to distinguish between two kinds of applications: server and clients. The server has the property of changing its transmission rate depending on the control information feedback sent by each client. The transmission and consumption rates

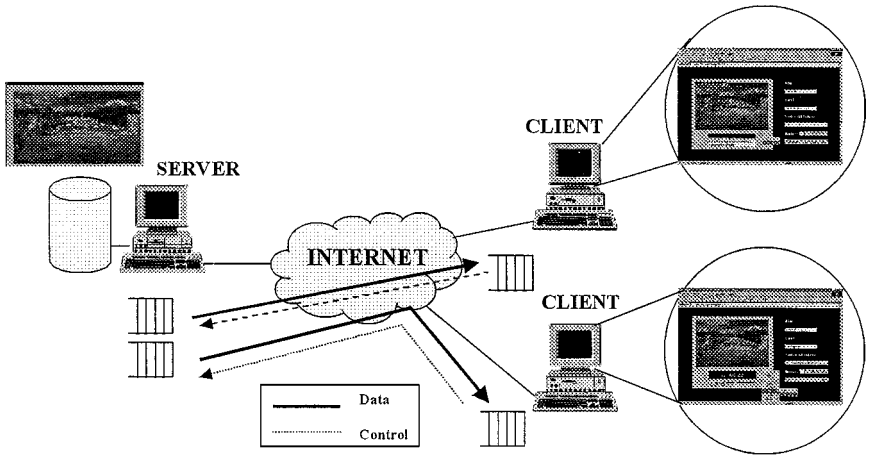

Figure 26. System architecture.

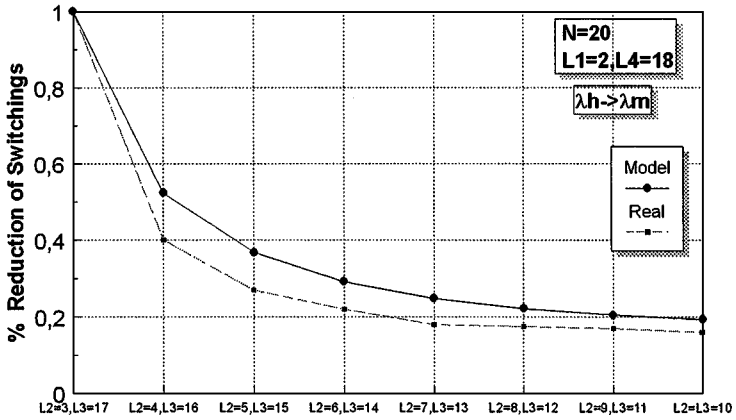

Figure 27. Reduction in the signaling traffic (real results vs. analytical model).

have been assumed to be constant with the following values: $\lambda_h = 22.5$; $\lambda_m = 15$; $\lambda_l = 7.5$; and $\mu = 15$ frames per second. The buffer size is $N = 20$ LDU's, and the threshold values are L1 = 2, L4 = 18. Both L2 and L3 are variables. The file used for the measurements was 5 Mbytes in length.

To validate our flow control model, we have considered two parameters: signaling traffic [6] and quality subjective evaluation [17]. Regarding signaling traffic, in figure 27 we qualitatively compare our results with results obtained by applying the analytical model. Clearly, the maximum number of changes in the transmission rate is achieved when no hysteresis is used at all—the first point in the graphics. With minimal hysteresial areas, the maximum value reduction is respectively around 40% and 50% for the real and analytical models. Less spectacular savings in signaling traffic are achieved when $L2 - L1 = L4 - L3 = 3$: around 25% and 38% respectively. We observe that the analytical model shows a smaller reduction in signaling than the real scenario. This is because the random variables in the real scenario have less standard deviation than the exponential distributions implicitly assumed in the analytical model showing lower limits in the signaling load reduction.

With regard to subjective evaluation, the evaluation of the synchronization protocol and flow control mechanism could be done using human perception of a multimedia presentation. This evaluation consists in the execution of several psycho-physic experiments (since multimedia presentations are generally directed to a human observer) which allow the subjective measurement of the quality of multimedia applications, and indirectly the performance of the synchronization protocol and flow control mechanism. The effects of delay, jitter, clock drift and the effect of the actions taken by the protocol should be considered.

The experiments and results obtained in [17] have served as a guide to design the measurement platform, and to develop the tests that had to be filled by the enquired. To carry out the subjective evaluation, a random population sample was chosen, trying to keep it balanced using the following variable or condition:

- Multimedia systems users.
- Multimedia systems non-users.

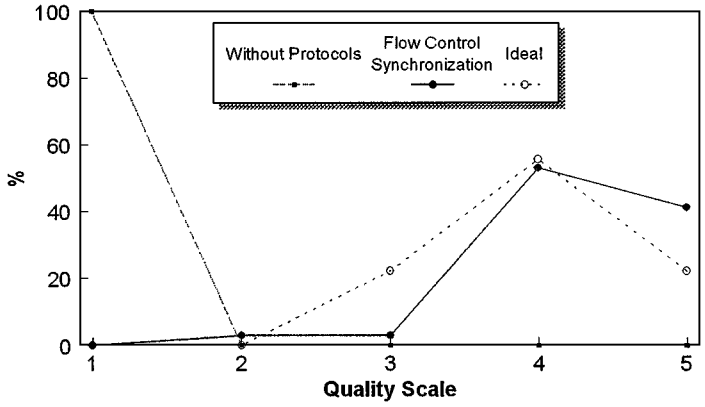

Figure 28. Video valuation.

Regarding the size of the population sample in subjective evaluation it is highly variable in the different studies analyzed by the authors. In the following results 20 people were used to carry out the experiments, 7 women and 13 men. None had done neither any psycho-physic experiment nor any study about multimedia applications.

The experiment consisted in the valuation of the application quality and compares several multimedia presentations *with* and *without* the execution of the flow control and synchronization protocols, and also in the *ideal* situation in which there was no underflow or overflow. Figure 28, represents the assessment of the quality measured using a scale in which 1 means "very bad" and 5 "very good", and the percentage corresponds to the people choosing that option. First of all it should be highlighted the clear difference that exists when the protocols are used or not (and the overflow and underflow is not avoided). In the late situation, all the subjects have evaluated the sequence with the worst quality. On the other hand, the achieved results with the synchronization and flow control protocols indicate the good performance of the mechanism. This means that the actions executed by

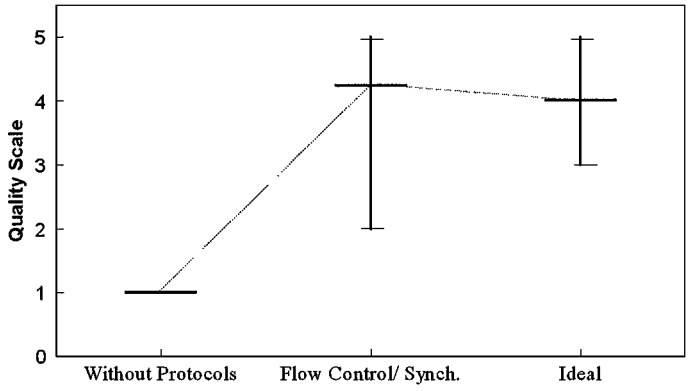

Figure 29. Maximum, minimum and mean of the video valuation.

the protocols have minimized the possibility that the subjects could perceive any disturbing effect.

In figure 29, the mean, minimum and maximum values are shown. It could be observed that the multimedia presentations with the protocols have a similar mean value to the mean value of the multimedia presentations completely synchronized and without overflow and underflow, although it is obvious that the values are not exactly so good.

6. Conclusions

For multimedia environments, we propose a flow control mechanism with hysteresis. The server receives the messages sent by the client in order to change the transmission rate. The decision to change the transmission rate is made according to the occupancy of the client buffer. To this end, two pairs of thresholds (L1, L2) and (L3, L4) have been used. L1 and L4 directly impact the underflow and overflow of the buffer. While L2 (>L1) and L3 (<L4) control the mean number of messages sent to the server.

When no hysteresis is used, $L2 - L1 = 1$ and $L4 - L3 = 1$, a maximum signaling rate is registered. A drastic saving is obtained when $L2 - L1 = 2$ and $L4 - L3 = 2$. The bigger the hysteresial areas ($L2 - L1 > 2$ and $L4 - L3 > 2$) the less significant is the reduction.

When several clients are served by the same server, a minimum transmission rate dispersion is achieved by not using hysteresis. However, the use of minimal hysteresial areas ($L2 - L1 = 2$, $L4 - L3 = 2$) does not significantly affect the dispersion rates—therefore obtaining a good compromise.

The analytical model has been compared with the results obtained by the measured performance in a real scenario. The conclusion is that our model captures the qualitative behavior of the real scenario. Therefore, our model can be used as an initial tool to evaluate the performance of real multimedia systems.

Other work in progress is the development and integration of the flow control and synchronization protocols with the widely used Internet RTP/RTCP and its performance evaluation when working in cooperation with the RSVP.

Acknowledgments

This work has been financed by Comisión Interministerial de Ciencias y Tecnología (Spain) (CICYT) under project numbers TIC96-0680 and TIC93-0990-CE.

References

1. J.C. Bolot and T. Turletti, "A rate control mechanism for a packet video in the internet," in Proc. IEEE INFOCOM'94, Toronto, June 1994, pp. 1216–1223.
2. V. Casares, "Variable bit rate voice using hysteresis thresholds," submitted for publication.
3. M. Esteve, C. Palau, and J.C. Guerri, "A synchronization service framework for XTP," in Proc. 20th Annual Conference on Local Computer Networks, Minneapolis, Oct. 1995, pp. 209–218.
4. J.F. Gibbon and T.D.C. Little, "The use of network delay estimation for multimedia data retrieval," IEEE Journal on Selected Areas in Communications, Vol. 14, No. 7, pp. 1376–1387, 1996.
5. J.C. Guerri, C. Palau, and M. Esteve, "Feedback-global protocol and the web: Framework and performance," in Proc. W3C Workshop Real-Time Multimedia and the World Wide Web, Sophia-Antipolis, France, Oct. 1996. Paper 6.

6. J.Y. Hui, E. Karasan, J. Li, and J. Zhang, "Client server synchronization and buffering for variable rate multimedia retrievals," IEEE Journal on Selected Areas in Communications, Vol. 14, No. 1, pp. 226–237, 1996.
7. S. Jacobs and A. Eleftheriadis, "Providing video services without quality of service guarantees," in Proc. W3C Workshop Real Time Multimedia and the World Wide Web, Sophia-Antipolis, France, Oct. 1996. Paper 20.
8. J. King, Computer and Communication Systems Performance Modeling, Prentice Hall, New York, 1990.
9. L. Kleinrock, Queueing Systems, Vol. 1, John Wiley, New York, 1975.
10. H. Kopetz and W. Ochsenreiter, "Clock synchronization in distributed real-time systems," IEEE Transactions on Computer C-38, pp. 933–939, 1987.
11. T.D.C. Little and A. Ghafoor, "Multimedia synchronization protocols for broadband integrated services," IEEE Journal on Selected Areas in Communications, Vol. 9, No. 9, pp. 1368–1382, 1991.
12. D. Mills, "Internet time protocol: The network protocol," IEEE Transactions on Communications, Vol. 39, No. 10, pp. 1482–1493, 1991.
13. S. Ramanathan and V. Rangan, "Adaptative feedback techniques for synchronized multimedia retrieval over integrated networks," IEEE/ACM Transactions on Networking, Vol. 1, No. 2, pp. 246–259, 1993.
14. V. Rangan and S. Ramanathan, "Designing an on-demand multimedia service," IEEE Communications Magazine, pp. 56–64, 1992.
15. S. Ross, Stochastic Process, John Wiley, New York, 1996.
16. R. Steinmetz, "Synchronization properties in multimedia systems," IEEE Journal on Selected Areas in Communications, Vol. 8, No. 3, pp. 401–411, 1990.
17. R. Steinmetz, "Human perception of Jitter and media synchronization," IEEE Journal on Selected Areas in Communications, Vol. 14, No. 1, pp. 61–72, 1996.
18. R. Steinmetz and K. Nahrstedt, Multimedia: Computing, Communications, and Applications, Prentice Hall, Upper Saddle River, NJ, 1995.

Juan C. Guerri Cebollada received his M.S. and Ph.D. (Dr. Ing.) degrees, both in Telecommunication Engineering, from the Universidad Politécnica de Valencia, in 1993 and 1997, respectively. He is a professor in the Escuela Técnica Superior de Ingenieros de Telecomunicación at the Universidad Politécnica de Valencia, and he works in the Distributed Real-Time Systems research group of the Departamento de Comunicaciones. He is currently in research and development projects for the application of multimedia and real-time technologies to industry, medicine, education and communications. Dr. Guerri is a member of IEEE. He achieved the best thesis award in Telematic Engineering from the COIT in 1997.

Manuel Esteve Domingo received his M.S. in Computer Engineering and Ph.D. in Telecommunication Engineering (Dr. Ing.) degrees, both from the Universidad Politécnica de Valencia, in 1989 and 1994, respectively. He is a professor in the Escuela Técnica Superior de Ingenieros de Telecomunicación at the Universidad Politécnica de

Valencia, and he leads the Distributed Real-Time Systems research group of the Departamento de Comunicaciones. He is currently in research and development projects for the application of multimedia and real-time technologies to industry, medicine, education and communications. Dr. Esteve is a member of IEEE.

Carlos E. Palau Salvador received his M.S and Ph.D. (Dr. Ing.) degrees, both in Telecommunication Engineering, from the Universidad Politécnica de Valencia, in 1993 and 1997, respectively. He is a professor in the Escuela Técnica Superior de Ingenieros de Telecomunicación at the Universidad Politécnica de Valencia, and he works in the Distributed Real-Time Systems research group of the Departamento de Comunicaciones. He is currently in research and development projects for the application of multimedia and real-time technologies to industry, medicine, education and communications. Dr. Palau is a member of IEEE and IASTED.

Vicente Casares Giner was born in Meliana (Valencia), Spain, on June 16, 1951. He obtained the Telecommunication Engineering degree in October 1974 from Escuela Técnica Superior de Ingenieros de Telecomunicación (ETSIT) de Madrid and the Dr. Engineering degree in September 1980 from ETSIT de Barcelona. During the period from 1974–1983 he worked on problems related to signal processing, image restoration, and propagation aspects of radiolink systems. In the first half of 1984 he was a visiting scholar at the Royal Institute of Technology (Stockhlom), dealing with digital switching and concurrent EUCLID for stores program control telephone systems. Since then he has been involved in queueing theory and teletraffic models. From 1992 to 1994 he worked in traffic and mobility models of MONET and ATDMA European RACE projects. From September 1994 to August 1995 he was a visiting scholar at WINLAB, Rutgers University. In 1991 he became professor at Universidad Politecnica de Catalunya. In September 1996 he moved to Universidad Politecnica de Valencia. His main interest is in the area of wireless systems, in particular random access protocols, voice and data integration, systems capacity and wireless ATM.